

Ultrasonic Transducers Composed of Functionally Gradient Piezoelectric Ceramics

S. Takahashi, S. Fukuda* and N. Ichinose***

Advanced Research Institute for Science and Engineering, Waseda University, 3-4-1, Okubo, Shinjuku-ku, Tokyo, 169-8555

Fax: 81-428-31-3136, e-mail: s-takahashi@shoichem.co.jp

*School of Science and Technology, Waseda University

Fax: 81-3-3200-2567, e-mail: ichinose@waseda.jp

**Kagami Memorial Laboratory, Material Science and Technology, Waseda University

Ultrasonic transducers used in measurement systems are required to have the capability of generating an ultrasonic pulse with a short time-waveform, i.e., a broadband frequency spectrum. In order to obtain the broadband transducer, ultrasound radiation characteristics for the piezoelectric ceramic transducer are studied by both computer simulation and experiment. Finite element method software ANSYS is used for the computer simulation. Piezoelectric ceramic transducers are fabricated by using ceramic green sheet technology. The composition of the ceramics is $(1-x)\text{Pb}(\text{Ni}_{1/3}\text{Nb}_{2/3})\text{O}_3-x\text{Pb}(\text{Zr}_{0.3}\text{Ti}_{0.7})\text{O}_3$ ($x=0.30\sim 0.50$). It has been shown that the transducer composed of functionally gradient piezoelectric ceramics with a ceramic backing radiates a single ultrasonic pulse. This ultrasonic pulse has a shorter time-waveform and a broader frequency spectrum compared with those for the usual transducer composed of uniform piezoelectric ceramics with a tungsten-epoxy backing.

Key words: ultrasonic transducer, piezoelectric ceramics, functionally gradient, short pulse-width, broadband frequency spectrum, ceramic backing

1. INTRODUCTION

Ultrasonic transducers composed of piezoelectric ceramics have been widely used in ultrasonic measurement systems such as nondestructive testing and medical diagnosis. Transducers are required to have the capability of generating a short time-waveform ultrasonic pulse, i.e., a broadband frequency spectrum, in order to achieve high-resolution ultrasonic imaging. Conventional ultrasonic transducers are basically composed of a uniform piezoelectric ceramic plate with a tungsten-epoxy backing bonded to the ceramic plate back surface. The ultrasonic pulse time-waveform of the conventional transducer, however, is not sufficiently short, because the transducer simultaneously generates a ultrasonic pulse at front and back surface of the ceramic plate upon impulse excitation and these pulses are repeatedly reflected between the two surfaces.

It has been known that a functionally gradient piezoelectric ceramic (FGM) plate generates a short time-waveform ultrasonic pulse. [1] Yamada et al. have succeeded in fabricating a FGM plate by giving a temperature gradient in the thickness direction for a fully-polarized piezoelectric ceramic plate and have found that the FGM plate with a ceramic backing, bonded together with an adhesive, generates a short time-waveform ultrasonic pulse. [2, 3]

In this study FGM transducer with a ceramic backing is fabricated by sintering a layer-structured ceramic green body without using any adhesive materials. [4, 5] Each individual layer is a green sheet composed of piezoelectric ceramic calcined powder with some organic binder, plasticizer and solvent. The composition of the calcined powder is different for each layer. Then, ultrasonic pulse characteristics radiated from this

transducer are experimentally evaluated. Ultrasonic pulse characteristics are also discussed using finite element method analysis. [6]

2. ULTRASOUND RADIATION PRINCIPLE FOR FGM TRANSDUCER

Ultrasound radiation principle for the conventional transducers composed of a uniform piezoelectric ceramic (non-FGM) plate is demonstrated in Figs. 1 (a), (b), (c), (d), (e) and (f). When the electric field E is

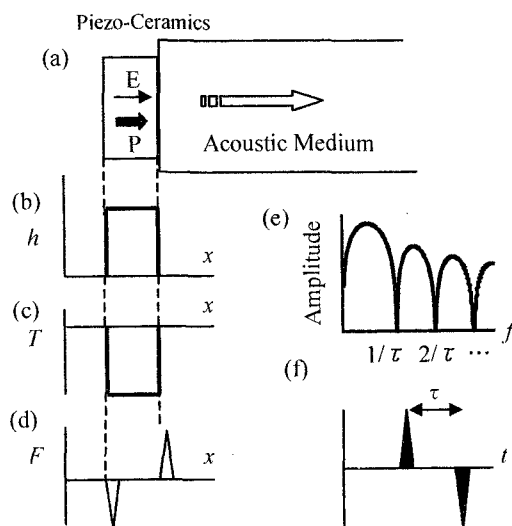


Fig. 1 (a) Electric field E and polarization P direction, distributions of (b) h -const. and (c) induced stress T , (d) volume force F , and ultrasound (e) frequency spectrum and (f) time-waveform for the non-FGM transducer.

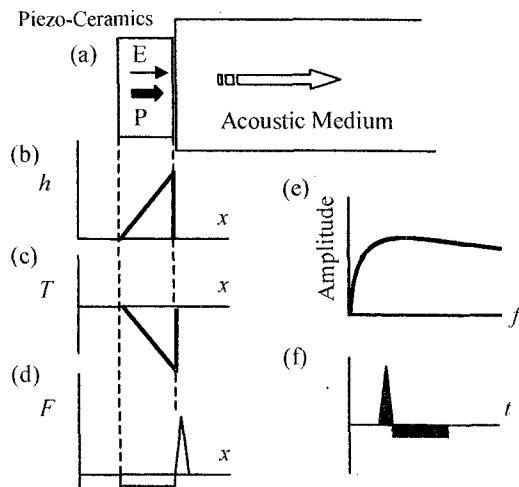


Fig. 2 (a) Electric field E and polarization P direction, distributions of (b) h -const. and (c) induced stress T , (d) volume force F , and ultrasound (e) frequency spectrum and (f) time-waveform for the FGM transducer.

applied parallel to the polarization P (a), the stress T ($T=h_{33}D$, h_{33} : piezoelectric h_{33} constant, D : electric displacement) is induced inside the ceramics (c). Therefore the volume force F ($F = \partial T / \partial x$) is concentrated at a front and back surface of the ceramic plate (d). Then, two ultrasonic pulses are simultaneously generated at a front and back surface and are launched into the acoustic medium with a time interval τ (f). Frequency spectrum of these ultrasonic pulses has many periodic attenuation poles (e).

Ultrasound radiation principle for the FGM transducer is shown in Figs. 2 (a), (b), (c), (d), (e) and (f). In this case the piezoelectric h_{33} constant has a gradient in the thickness direction between one face to the other (b), so that the induced T has a gradient (c) and the F concentrates only at the front surface of the ceramic plate (d). Then, a single pulse is launched into the acoustic medium (f) and its frequency spectrum becomes very broad (e). That is, the FGM transducer has a broadband frequency spectrum compared with the non-FGM one.

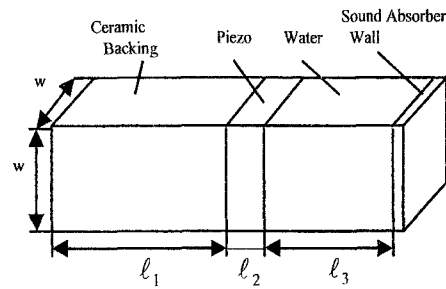


Fig. 3 Model for the finite element method analysis.

3. FINITE ELEMENT METHOD ANALYSIS

Three dimension analysis for the transient response of piezoelectric-acoustic system was carried out using the finite element method software ANSYS. The model used for the analysis is shown in Fig. 3.

Non-polarized piezoelectric ceramics were defined as a backing. Length of a backing l_1 , piezoelectric ceramics l_2 and acoustic medium (water) l_3 were

20mm, 1.54mm and 5mm, respectively. The end surface of the acoustic medium was defined as a sound absorber wall in order to suppress the reflection. Material constants used here were as follows: dielectric constant $\epsilon_{33}^S=2660$, elastic stiffness $c_{33}^D=11.9 \times 10^{10}$ N/m² and density $\rho=8 \times 10^3$ kg/m³. Applied pulse voltage had a triangle shape with a 20 V height and a 50 ns width.

The gradient of piezoelectric h_{33} constant was represented by 16 piezoelectric elements having a different h_{33} value one another as shown in Figs. 4 (a), (b) and (c). Three types of piezoelectric gradient such as convex-FGM (a), linear-FGM (b) and concave-FGM (c) were examined. The following functions were used for the individual gradient curve fitting:

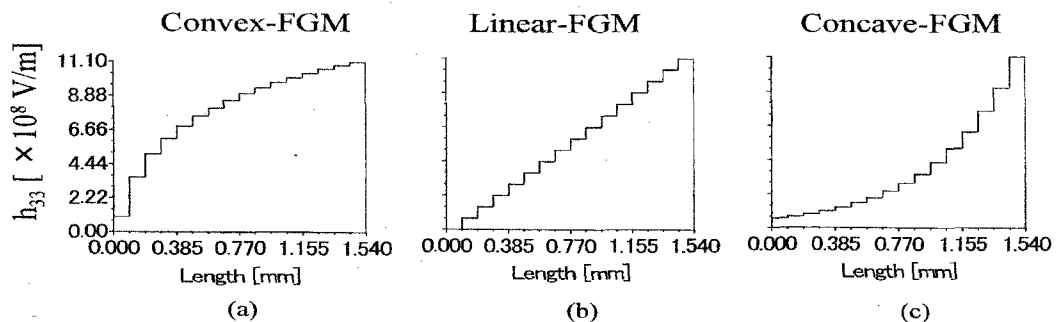


Fig. 4 Types of piezoelectric gradient. (a) Convex-FGM, (b) linear-FGM and (c) concave-FGM.

$$h_{33}(z) = h_{33} \left\{ 1 + \frac{1}{\alpha \ell_2} (\ln z - \ln \ell_2) \right\}, \quad (1)$$

$$= \frac{h_{33}}{\ell_2} z, \quad (2)$$

$$= h_{33} \exp\{\alpha(z - \ell_2)\}, \quad (3)$$

$$\alpha = 2$$

Figures 5 (a), (b), (c) and (d) show the time-waveform simulation results for the non-FGM, the convex-FGM, the linear-FGM and the concave-FGM transducer, respectively. For the non-FGM transducer, two ultrasonic pulses with the inverse phase each other are radiated to the acoustic medium. The time interval τ between two pulses is about $0.4 \mu\text{s}$ which corresponds to the ultrasonic wave traveling time across the piezoelectric plate thickness. Consequently, the earlier pulse is the pulse radiated from the front surface of the plate and the later is the pulse radiated from the back surface. It is clear that the pulse radiated from the back surface is reduced for the FGM transducer compared with the non-FGM transducer.

Figures 5 (a'), (b'), (c') and (d') show the frequency spectrum simulation results for the non-FGM, the convex-FGM, the linear-FGM and the concave-FGM transducers, respectively. There are many attenuation poles in the frequency spectrum for the non-FGM transducer. The frequencies of these attenuation poles correspond to the anti-resonant frequencies of the odd-order vibration modes. Depth of the attenuation pole is reduced for the FGM transducers. Frequency spectrum for the concave-FGM transducer is the smoothest of all and has broadband frequency characteristics.

4. EXPERIMENTS

4.1 Sample Preparation

Figure 6 shows a phase diagram of pseudo-ternary solid solution system of ferroelectric ceramics

$\text{Pb}(\text{Ni}_{1/3}\text{Nb}_{2/3})\text{O}_3\text{-PbZrO}_3\text{-PbTiO}_3$. Ceramics with the compositions of $(1-x)\text{Pb}(\text{Ni}_{1/3}\text{Nb}_{2/3})\text{O}_3\text{-xPb}(\text{Zr}_{0.3}\text{Ti}_{0.7})\text{O}_3$ ($x=0.30\sim 0.50$) were used for the fabrication of FGM transducers. Figure 7 represents experimental values of the piezoelectric h_{33} constant and the theoretical Ti concentration as a function of composition x . For the ceramics with $x=0.30$, $h_{33}=0$, and the value of h_{33} increases with increasing x .

Fabrication procedures for the FGM transducer with a ceramic backing is shown in Figs. 8 (a) and (b). The procedures are almost the same as those for the multilayer piezoelectric ceramic actuators. [7] Ceramic green sheets composed of ceramic calcined powder with some organic binder, plasticizer and solvent are laminated and pressed together into the green body (a). The part that will be the FGM after sintering consists of green sheets with various composition x . The top green sheet has a composition of $x=0.50$, and the bottom has that of $x=0.30$. The part that will be a ceramic backing after sintering, however, consists only of the green sheets with $x=0.30$. The Pt metal paste layer that will be the inner electrode after sintering is inserted in the green body. The FGM transducer is obtained co-firing the above green body (b).

4.2 Piezoelectric Gradient Evaluation

Compositional gradient was evaluated by the EPMA analysis. The Ti concentration is shown as a function of depth from the ceramic surface in Fig. 9. The Ti concentration is almost constant from the surface to the depth of about $350 \mu\text{m}$, however it then monotonically decreases with the depth up to the inner electrode position ($\sim 850 \mu\text{m}$). The gradient of h_{33} can be estimated from the relationship between h_{33} and Ti concentration (Fig. 7) and the estimation result is also shown in Fig. 9 with a dotted line. It is clear that the h_{33} value has a linear gradient.

Figures 10 (a) and (b) show the electrical admittance characteristics focused on the thickness vibration mode for the non-FGM disk with the composition of $x=0.50$ and for the linear-FGM disk, respectively.

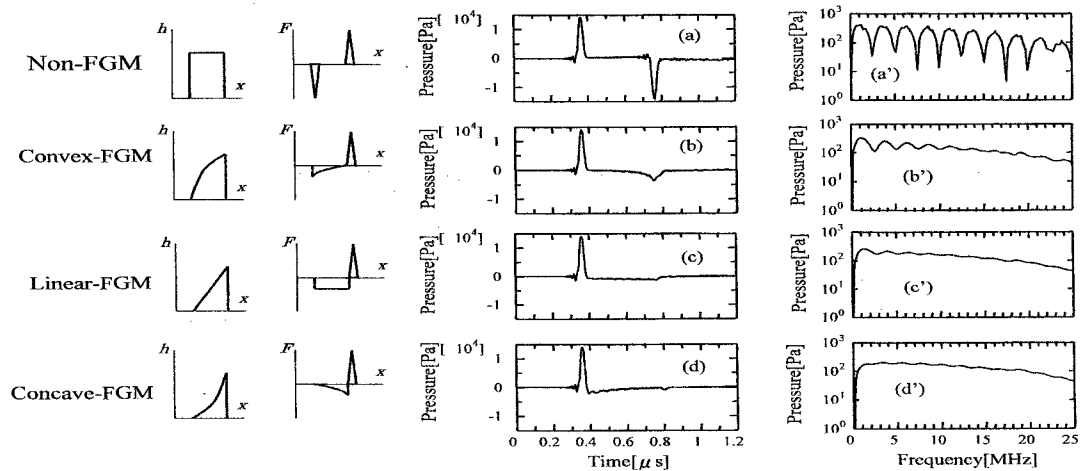


Fig. 5 Simulation results. Time-waveforms for the (a) non-FGM, (b) convex-FGM, (c) linear-FGM and (d) concave-FGM. Frequency spectra for the (a') non-FGM, (b') convex-FGM, (c') linear-FGM and (d') concave-FGM.

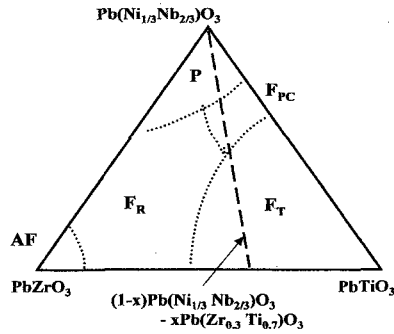


Fig. 6 Phase diagram for the pseudo-ternary solid solution system $\text{Pb}(\text{Ni}_{1/3}, \text{Nb}_{2/3})\text{O}_3\text{-PbZrO}_3\text{-PbTiO}_3$.

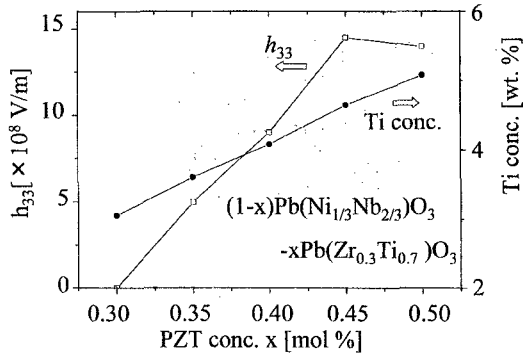


Fig. 7 Observed values for the piezoelectric h_{33} constant and theoretical values for the Ti concentration as a function of composition x .

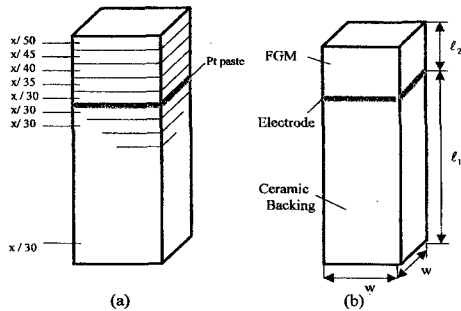


Fig. 8 Procedures for the FGM transducer. (a) Before sintering and (b) after sintering.

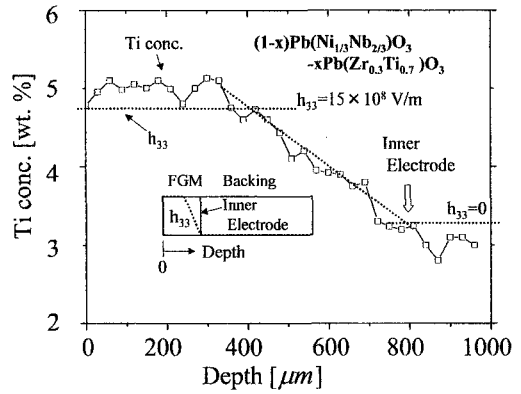


Fig. 9 Observed values for the Ti concentration and estimated values for the h_{33} as a function of depth from the surface of the ceramics.

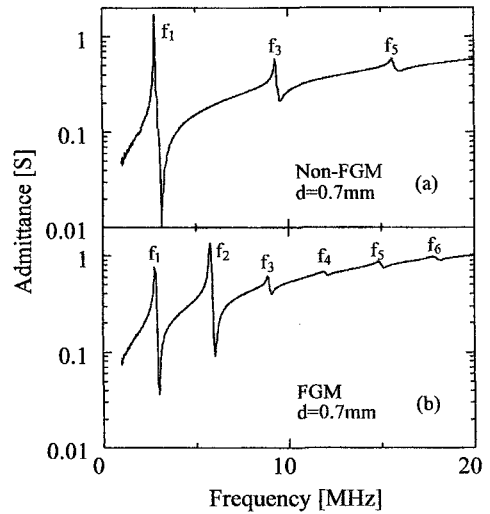


Fig. 10 Admittance characteristics for the (a) non-FGM disk and (b) FGM disk.

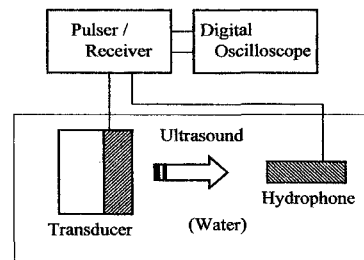


Fig. 11 Experimental setup for the ultrasonic radiation measurements.

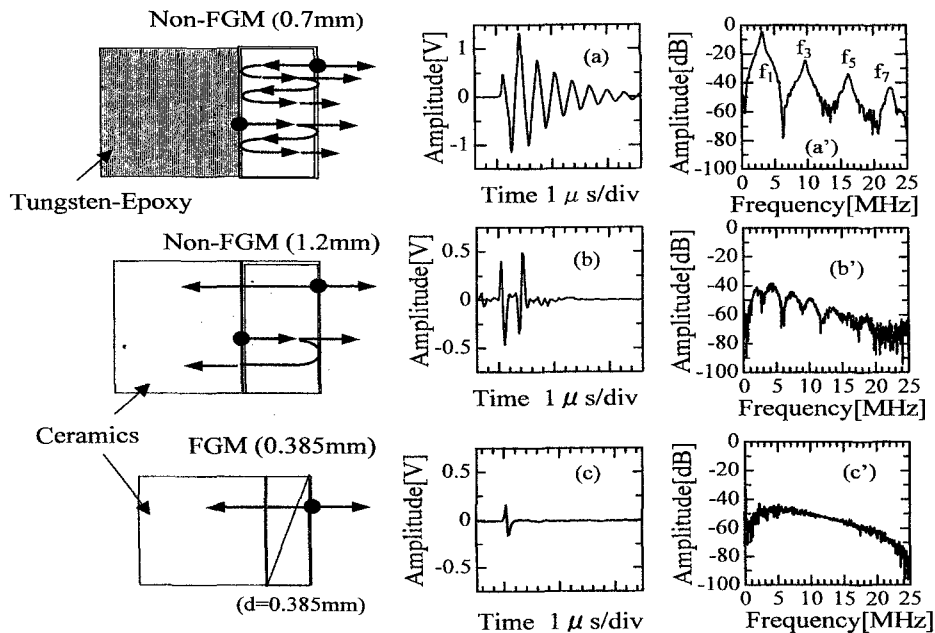


Fig. 12 Experimental results for ultrasonic radiation characteristics. Time-waveforms for the (a) non-FGM with a tungsten-epoxy backing, (b) non-FGM with a ceramic backing and (c) FGM with a ceramic backing transducer. Frequency spectra for the (a') non-FGM with a tungsten-epoxy backing, (b') non-FGM with a ceramic backing and (c') FGM with a ceramic backing transducer.

Thickness of the two ceramic disks is 0.7 mm. As is well known, the resonant responses for the even-order vibration mode appear in the non-FGM disk. It is noted, however, that both the even- and odd-order mode resonant responses appear in the FGM disk. [8] These results indicate that the FGM disk examined here has a gradient not only for the ceramic composition but also for the piezoelectric parameters.

4.3 Ultrasound Radiation Measurements

The experimental setup for the ultrasonic wave measurements is shown in Fig. 11. The transducer was driven in water by applying a negative spike-shaped pulse voltage using the pulser-receiver (Panametrics 5800PR). The launched ultrasonic wave was received by the hydrophone probe (Specialty Engineering Associates PVDF-z44-100). The time-waveform of the ultrasound and its frequency spectrum were observed using the digital oscilloscope (Hewlett Packard HP54810A) equipped with a fast Fourier transform (FFT) function.

The time-waveform and frequency spectrum for the non-FGM transducer with a tungsten-epoxy backing are shown in Figs. 12 (a) and (a'), respectively. Thickness of the non-FGM plate is 0.7 mm. The time-waveform shows long trailing pulses and the amplitude of the frequency spectrum has attenuation poles at the even-order vibration mode anti-resonant frequencies. Figures 12 (b) and (b') show the results relating to the non-FGM transducer with a ceramic backing. Thickness of the non-FGM part is 1.2 mm. It is clear that the reflection wave from the boundary between piezoelectric part and a ceramic backing is completely suppressed. Figures 12 (c) and (c') show the results relating to the FGM transducer with a ceramic backing. Thickness of the FGM part is 0.358 mm. The result indicates that this

transducer generates a single pulse and its frequency spectrum is very wide and smooth.

5. CONCLUSION

Ultrasonic transducers composed of functionally gradient piezoelectric ceramics with a ceramic backing were studied by computer simulation and experiments. Finite element method software ANSYS was used for the computer simulation and three types of piezoelectric gradient such as the convex-, linear- and concave-type were examined. Simulation results indicate that the transducer having the concave- or linear-type piezoelectric gradient radiates a single ultrasonic pulse which has a broadband frequency spectrum.

Linear-type functionally gradient piezoelectric ceramic transducer with a ceramic backing was experimentally fabricated using ceramic green sheet technology. As the piezoelectric ceramics, $(1-x)\text{Pb}(\text{Ni}_{1/3}\text{Nb}_{2/3})\text{O}_3-x\text{Pb}(\text{Zr}_{0.3}\text{Ti}_{0.7})\text{O}_3$ ($x=0.3 \sim 0.50$) was used. Gradient of piezoelectric parameter was realized by sintering the green body composed of green sheets with various composition x . Piezoelectric gradient was estimated by the Ti concentration analysis and the electric admittance measurements. The transducer is confirmed to radiate a single ultrasonic pulse with a broadband frequency spectrum.

Acknowledgements

This work was supported in part by Special Coordination Funds of the Ministry of Education, Culture, Sports, Science and Technology of the Japanese Government.

The authors wish to thank Dr. K. Yamada from Tohoku University, and Dr. T. Yamamoto and Dr. H. Okino from National Defense Academy for their useful discussion.

6. REFERENCES

- [1] A. F. Broun and J. P. Weight, *Ultrasonics*, July, 161-167 (1974).
- [2] K. Yamada, D. Yamazaki and K. Nakamura, *Jpn. J. Appl. Phys.*, **40**, L49-L52 (2001).
- [3] J. K. Yamada, D. Yamazaki and K. Nakamura, *Proc. 2000 IEEE Ultrason. Symp.*, 1017-1020 (2000).
- [4] T. Kawai and S. Miyazaki, *J. Ceram. Soc. Japan*, **98**, 900-904 (1990). [in Japanese]
- [5] S. Takahashi, N. Miyamoto and N. Ichinose, *Jpn. J. Appl. Phys.*, **41**, Part 1, No. 11B, 7103-7107 (2002).
- [6] S. Fukuda, S. Takahashi and N. Ichinose, *Technical Report IEICE*, US2003-85, 1-6 (2003). [in Japanese]
- [7] S. Takahashi, A. Ochi, M. Yonezawa, T. Yano, T. Hamatsuki and I. Fukui, *Ferroelectrics*, **50**, 181-184 (1983).
- [8] K. Yamada, J. Sakamura and K. Nakamura, *IEEE Trans. UFFC*, **48**, 613-616 (2001).

(Received December 23, 2004; Accepted January 31, 2005)